Open Journal of Acoustics, 2011, 1, 63-69
doi:10.4236/oja.2011.13008 Published Online December 2011 (http://www.SciRP.org/journal/oja)

Towards Earthquake Shields: A Numerical Investigation of Earthquake Shielding with Seismic Crystals

Baris Baykant Alagoz[1], Serkan Alagoz[2]
[1]*Department of Electric-Electronics Engineering, Inonu University, Malatya, Turkey*
[2]*Department of Physics, Inonu University, Malatya, Turkey*
E-mail: *baykant.alagoz@inonu.edu.tr*
Received October 10, 2011; *revised November* 14, 2011; *accepted November* 24, 2011

Abstract

Authors numerically demonstrate that the seismic surface waves from an earthquake can be attenuated by a seismic crystal structure constructed on the ground. In the study, seismic crystals with a lattice constant of kilometer are investigated in the aspect of band gaps (Stop band), and some design considerations for earthquake shielding are discussed for various crystal configurations in a theoretical manner. Authors observed in their FDTD based 2D wave simulation results that the proposed earthquake shield can provide a decreasing in magnitude of surface seismic waves. Such attenuation of seismic waves might reduce the damage in an earthquake.

Keywords: Earthquake Shielding, Seismic Metamaterials, Seismic Wave Attenuation, Band Gap Analysis

1. Introduction and Preliminaries

In recent research about photonic, phononic and sonic crystals, band gaps were observed in the band structure characteristics of crystals with various lattice geometries [1-20]. As crystal structures exhibit very low transmission in the frequencies within band gaps, they were also referred to as "stop bands." Band gaps appear in the wave transmission spectrum when a homogenous wave propagation medium turns into an inhomogeneous medium with periodic defects. Those periodical defects in the medium disturb the wave propagation at certain frequency groups, which make up the so-called band gap. In general, the periodical defects in a medium are commonly called scatterers and the medium in which the wave propagates is called the host material of the crystal structure.

In order to form such a periodically inhomogeneous medium, photonic crystals, used for electromagnetic waves, are composed of periodically modulated dielectric materials [9-12]; sonic crystals for acoustic waves are mostly composed of periodic arrays of solid rods in the air [1,3-5] and phononic crystal are made of solid or liquid host material with a periodic inhomogenization [15-17]. For a seismic crystal implementation, in our study, we preferred periodic holes in the ground as the scatterers and the ground itself as the host material. A representation of a 2D seismic crystal structure and its relevant design parameters is given in **Figure 1**. The hole scatterer-solid host configurations and their full band gap effect were demonstrated for surface acoustic waves on two-dimensional phononic crystal in the sub-meter scales, such as a piezoelectric phononic crystals [15-17]. As a result of scalability features of two dimensional crystal lattice with respect to wavelength (a/λ is constant), the similar band gap effects can be obtained for the seismic waves via a larger crystal implementation in the scales of kilometers [14]. This idea was our basic motivation in this theoretical work.

In general notation, the distance between the centers of the cylindrical scattering materials is referred to as the lattice constant and denoted by a, and radius of the cylindrical scattering material is denoted by r. The parameter h is the height of the holes and λ represents the wavelength.

Band gap properties of crystal structures have been used practically in the application of wave isolation in a selected frequency band [5,6,8,18,19]. In a similar fashion, we numerically investigate crystal structures built on the ground in order to attenuate the longitudinal ground vibrations propagating on the surface of the earth by means of band gaps. We employed the hole-ground type crystal structures to be a sort of seismic crystal and applied them towards isolating a region from seismic waves, *i.e.*, to earthquake shielding. Another technique to isolation, recently made progress, is to cloaking method

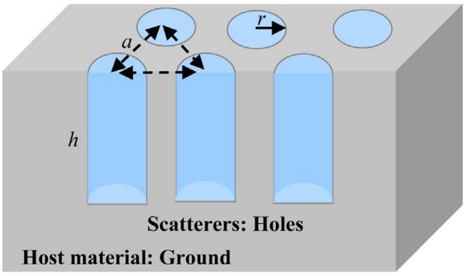

Figure 1. Representation of 2D seismic crystal.

that can isolate a region by steering wave envelopes around to isolated region instead of attenuating their amplitudes [20,21]. However, a wide-band cloaking technique [21] should be developed for the efficient applications.

In order to theoretically demonstrate the wave attenuation effect in the proposed crystal structures, we applied the Finite Difference Time Domain (FDTD) method, which is a very common numerical analysis technique used in acoustic wave simulations in inhomogeneous materials [1,3]. In this simulation method, seismic waves in the ground were assumed to travel as compression and decompression fields in a granular structure via displacements of granules. In order to model this type of the wave propagation numerically, a linear wave equation system based on parameters of granule (particle) velocity and pressure field were solved for a two-dimensional plane by using the FDTD method. In our earthquake simulations, a narrow band vibration signal containing very low sampled frequency components up to 10 Hz was generated in the pressure field. By using spatiatemporal solution of wave propagation, the Richter scaled map of the ground vibration, which is composed of the maximum instant granule velocities, was obtained to show the efficiency of the earthquake shielding. Additionally, wavelength responses of some basic seismic crystal configurations were analyzed to give a comparison of several crystal configuration types.

2. Method

2.1. Theoretical Background

To do a numerical analysis of wave propagation on the surface layer of the Earth, the ground is assumed to be composed of dynamic tiny granular structures as illustrated in **Figure 2**. In this system, the pressure in a unit volume of the ground is dependent on the density of the volume and it can be expressed as a function of the density, $P = P(\rho)$. Thickness of surface layer is assumed to be narrow enough to ignore variation in density ρ depending on the gravity.

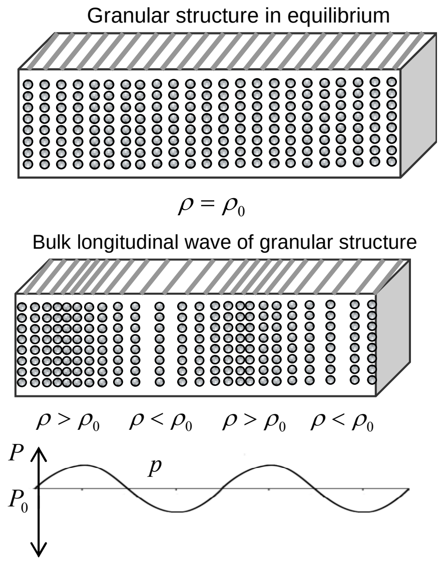

Figure 2. Granule displacements and corresponding pressure field in one dimension.

When the granules forming the ground are allowed to a short directional displacement around their resting location, the density will exhibit a small variation around an equilibrium density ρ_0. In this case, by applying a linear approximation, the pressure function $P(\rho)$ can be written as,

$$P \cong P_0 + \left(\frac{\partial P}{\partial \rho}\right)_{\rho_0} (\rho - \rho_0) \tag{1}$$

Therefore the deviation in pressure from the equilibrium pressure of the ground result in the forces that move granular structures in ground, it will be meaningful to consider the pressure deviation, $p = P - P_0$, in the analysis of seismic waves. Hence, considering the Equation (1), the pressure field of the seismic wave can be reorganized as

$$p = K_o s \tag{2}$$

where the parameter K_0 is bulk modulus of media and expressed as $K_0 = \rho_0 \left(\partial P/\partial \rho\right)_{\rho_0}$ and s denotes squeezing rate and defined as $s = (\rho - \rho_0)/\rho_0$.

In this system, the granule displacements even in short distances lead to alternations in local pressure field variations and result in compression (high pressure) and decompression (low pressure) fields inside the ground as represented in **Figure 2**. Meanwhile, the gradient in the pressure fields causes new granule motions. This mutual interaction between the pressure and the granule displacements results in wave propagation through the medium. Since this motion of granules is the small in magnitudes, the Euler equation, which is also known as the linear inviscid force equation, can be used to model this phenomenon [25].

$$\nabla p = -\rho_0 \frac{\partial \boldsymbol{V}}{\partial t} \tag{3}$$

where the vector $\boldsymbol{V}$ is the velocity of the granules. On the other hand, the motion of granules in a unit volume of ground must comply with the mass continuity equation and it was expressed as [25]

$$\frac{\partial \rho}{\partial t} + \boldsymbol{\nabla} \cdot (\rho \boldsymbol{V}) = 0 \tag{4}$$

Solid granules have quite low viscosity, so the ground can be assumed to be a inviscid media. ($s \ll 1$) In that case, the mass continuity equation for linear mediums can be obtained as,

$$\left(\frac{\partial (p/K_0)}{\partial t}\right) + \boldsymbol{\nabla} \cdot \boldsymbol{V} = 0 \tag{5}$$

Here, the ρ density of medium is considered as $\rho = \rho_0 (1+s)$ and s is written as $s = p/K_0$ according to Equation (2). If the Equations (3) and (5) are reorganized for a medium, where variation in bulk modulas in temporal domain are negligibly small, we obtains the following linear wave equation system,

$$\frac{\partial \boldsymbol{V}}{\partial t} = -(1/\rho_o)\nabla p \quad \text{and} \quad \frac{\partial p}{\partial t} = -K_0 \boldsymbol{\nabla} \cdot \boldsymbol{V}, \tag{6}$$

The Equation (6) was normalized by the material parameters of a simple uniform medium which will be the ground in our case. The following normalized linear wave equation system is obtained for the wave motion simulation in a inhomogeneous media:

$$\frac{\partial \boldsymbol{v}}{\partial u} = -\rho \nabla p \quad \text{and} \quad \frac{\partial p}{\partial u} = -K \boldsymbol{\nabla} \cdot \boldsymbol{v}, \tag{7}$$

where $\boldsymbol{v}$ denotes the normalized granule velocity and p is the pressure. The material parameters of inhomogeneous structures are described by the normalized medium density, $\rho = \rho_0/\rho_s$, and the normalized bulk modulus, $K = K_s/K_o$. Here, ρ_0 is the density of the host material and K_0 is the bulk modulus of the host material. ρ_s and K_s are the corresponding parameters for the scattering material.

To obtain an FDTD based numerical solution of (7), finite difference equations are derived for the spatial plane seen in **Figure 3(a)**. The calculation of granule velocity vectors, defined as $\boldsymbol{v} = [v_x \; v_y]$, is done by using discrete finite difference formulas:

$$v_x^{n+\frac{1}{2}}\left(i+\frac{1}{2}, j\right) = v_x^{n-\frac{1}{2}}\left(i+\frac{1}{2}, j\right) - \rho\left(i+\frac{1}{2}, j\right) R_x \left[p^n(i+1, j) - p^n(i, j) \right] \tag{8}$$

$$v_y^{n+\frac{1}{2}}\left(i, j+\frac{1}{2}\right) = v_y^{n-\frac{1}{2}}\left(i, j+\frac{1}{2}\right) - \rho\left(i, j+\frac{1}{2}\right) R_y \left[p^n(i, j+1) - p^n(i, j) \right] \tag{9}$$

The calculation of the pressure field is made with the following discrete finite difference formula:

$$\begin{aligned} p^{n+1}(i,j) = {} & p^n(i,j) - K(i,j) R_x \cdot \left[v_x^{n+\frac{1}{2}}\left(i+\frac{1}{2}, j\right) - v_x^{n+\frac{1}{2}}\left(i-\frac{1}{2}, j\right) \right] \\ & - K(i,j) R_y \left[v_y^{n+\frac{1}{2}}\left(i, j+\frac{1}{2}\right) - v_y^{n+\frac{1}{2}}\left(i, j-\frac{1}{2}\right) \right] \end{aligned} \tag{10}$$

For the stability of the wave propagation in FDTD simulation, R_x and R_y parameters should satisfy the Courant condition [1] and expressed as,

$$R_x = \frac{\Delta u}{\Delta x} \quad \text{and} \quad R_y = \frac{\Delta u}{\Delta y}. \tag{11}$$

The Δx and Δy represent unit distances in the spatial domain and Δu is the normalized unit time that is defined as $\Delta u = c\Delta t$. Here, Δt and c is the unit time increment and wave velocity, respectively.

Swells on the surface level of the ground accompany compressed and decompressed fields in the ground. For the sake of simplicity, we used a linear modeling for the ground swelling for a cubic unit volume on the surface layer of ground seen in **Figure 3(b)**. The rise in upper surface of the unit volume (Δh) is considered to be proportional to deviation of density from its equilibrium value, that is, $\Delta h = \xi(\rho - \rho_0)$. The parameter ξ, expressed as $\partial h/\partial \rho$, is the swelling to density rate of the unit volume. The Equation (2) can be written in the form of $p = c^2 (\rho - \rho_0)$ owning to $c^2 = K_0/\rho_0$. In that case, the change in the surface level of a unit volume can be estimated by:

$$\Delta h = \alpha p \tag{12}$$

Here, $\alpha = \xi/c^2$ is the swelling coefficient.

Equations (7) were previously applied in the simulations of acoustic wave propagation in sonic crystals [1, 3,4]. In our work, we see that seismic waves can be supposed as the earthquakes sounds propagating through the ground and many properties observed in acoustic wave propagation in a solid media, such as the reflection, the refraction and the attenuation of waves, are also valid in the seismic wave propagation on the ground. In the following sections, we will numerically analyze frequency-selective attenuation effects of periodically defected grounds on the seismic wave propagation.

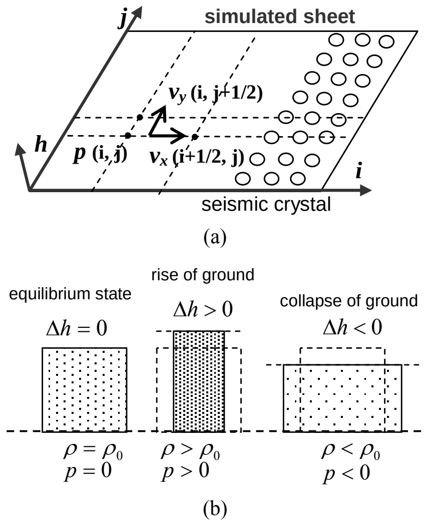

Figure 3. (a) Simulation plane and corresponding parameters used in discrete solution points grid; (b) Ground swelling by the pressure.

2.2. Earthquake Simulation Results

In this section, FDTD based simulation results of earthquake shielding are presented in the Richter scale, which is the logarithm of the maximum displacement in microns ($M = \log \Delta x_{micron}$). In the simulation, a rectangular sheet representing the host material was stimulated by a signal of a pressure field (p) containing multi-frequency components as illustrated in **Figure 4**. This signal was generated by the following function,

$$\begin{aligned} Ps(n) &= \sin(\pi \cdot n) + \sin(2\pi \cdot n) + \sin(4\pi \cdot n) \\ &+ \sin(6\pi \cdot n) + \sin(8\pi \cdot n) \\ &+ \sin(10\pi \cdot n) + \sin(20\pi \cdot n) \end{aligned} \tag{13}$$

where n is the simulation time index. The simulation time can be expressed as $u = n \cdot \Delta u / c$. The basic steps of the algorithm are presented in **Figure 5**.

In the proposed FDTD based wave simulations, the wave velocity in the host material (c) is to 3000 m/sn. For the scattering material, the normalized medium density ρ was set to 10 and the normalized bulk modulus K to 0.1. The Δx and Δy unit distances in spatial domain were set to 40 m and Δu normalized unit time was set to 4.66×10^{-3} second. By considering Equation (12), the pressure wave pattern (p) also forms a map of the ground swelling (Δh) for $\alpha = 1$.

Vibration maps in Richter scale are composed of the norm of the maximum instant velocity vector parallel to ground. It is calculated by using the following formula,

$$V_{\max}(i,j) = \max\left(\sqrt{\left(v_x^{n-1/2}(i,j)\right)^2 + \left(v_y^{n-1/2}(i,j)\right)^2} \right) \tag{14}$$

$$\text{for} \quad n \in \left[0, n_{sim}\right]$$

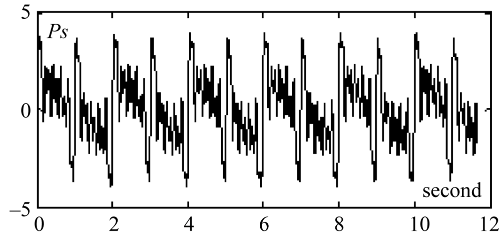

Figure 4. Multi-frequency pressure signal produced at the earthquake center in the simulation.

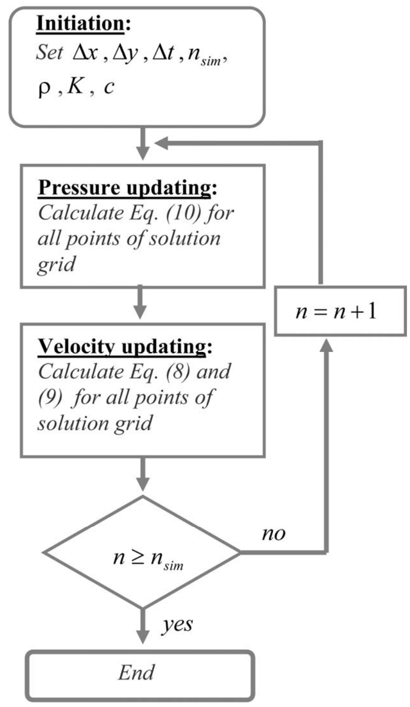

Figure 5. Basic steps of algorithm.

where, n_{sim} specifies simulation duration and $V_{\max}$ is the maximum displacement in a second.

Simulation results for seismic crystal types with various scatterer geometries and lattice configurations are given in **Figure 6**. A decreasing in magnitude of vibration is apparent behind the seismic crystals when compared with the vibration magnitude in the unshielded region. Elliptic scatterers [22] are seen to exhibit better performance of isolating seismic waves. A serious disadvantage of the circular scatterers for the application of earthquake shielding is that the crystals with circular scatters can exhibit wave focusing effect within a certain frequency band [23,24].

2.3. Obtaining Maximum Acceleration Map from the FDTD Simulations

Maps of maximum granule acceleration are useful in

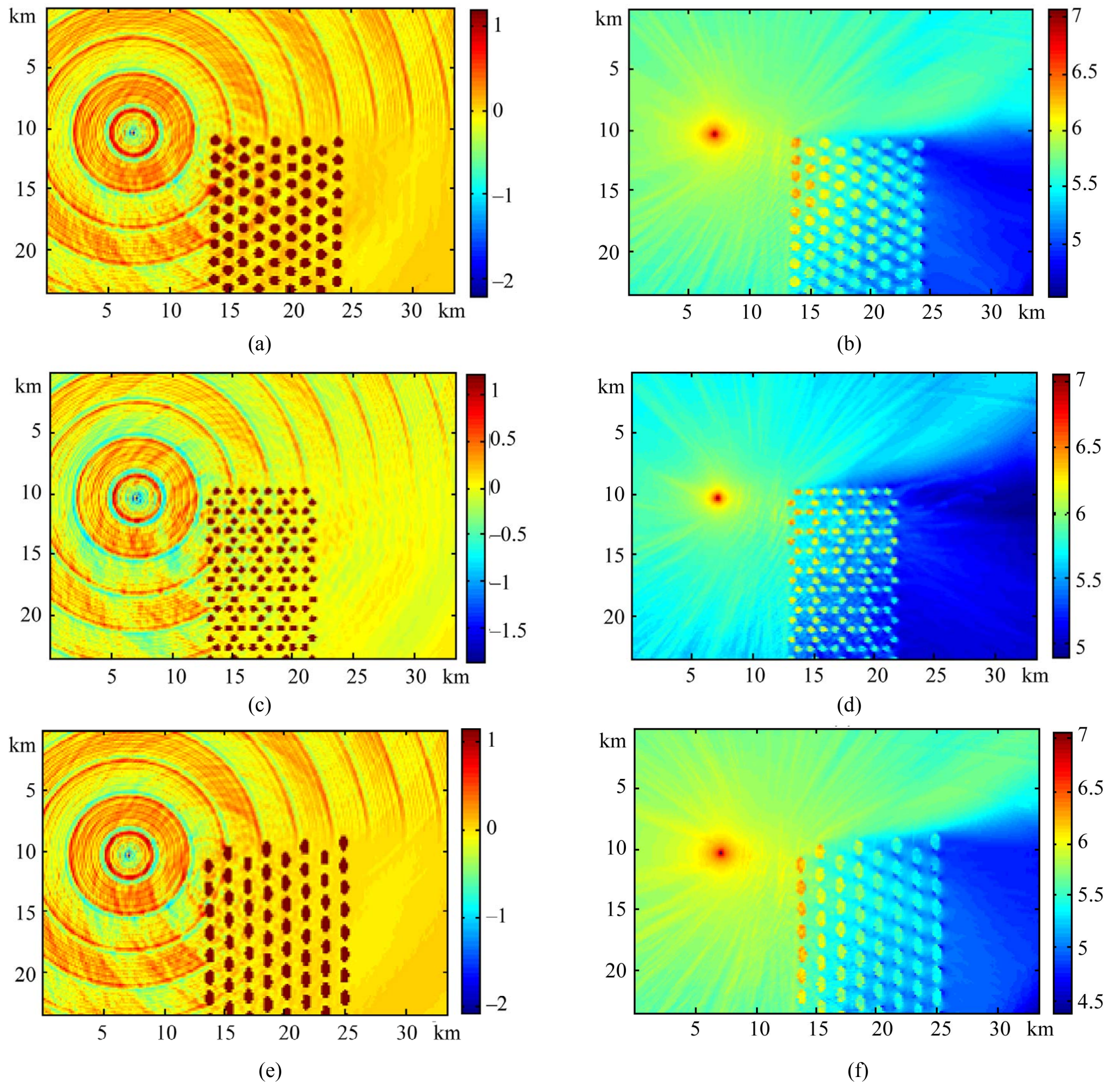

Figure 6. Pressure wave (*p*) pattern images and vibration maps in Richter scale for triangular lattice of circular scatterer (a, b), honeycomb lattice of circular scatterer (c, d), triangular lattice of elliptic scatterer (e, f).

estimating the destructive forces applied on buildings by seismic waves. The granule acceleration can be simply expressed as $\boldsymbol{a} = \partial \mathbf{v} / \partial t$. By applying the backwards difference to derivatives, the amplitudes of the maximum granule acceleration are calculated in the discrete form by the following formula,

$$A_{\max}(i,j) = \max\left\{ \frac{1}{\Delta u} \left(\left(v_x^{n+1/2}(i,j) - v_x^{n-1/2}(i,j) \right)^2 + \left(v_x^{n+1/2}(i,j) - v_y^{n-1/2}(i,j) \right)^2 \right)^{1/2} \right\} \quad (15)$$

for $n \in [0, n_{sim}]$

Figure 7 shows an estimate of the maximum acceleration maps. In these figures, the effect of the seismic crystal on the acceleration of the ground is clearly seen.

2.4. Wavelength Response Analysis for Various Seismic Crystals

In this section, the wavelength response of seismic crystal with various lattice configurations and scatterer shapes are investigated. For this purpose, we recorded pressure values ($p_{0,\lambda}(n)$, $p_{1,\lambda}(n)$) in the simulation, which is done for each sampled wavelength in the seismic spectrum. The $p_{1,\lambda}$ array stores the pressure data from the point in the shielded side and $p_{0,\lambda}$ stores the pressure data at the same point in the absence of the crystal. The reduction rate of shielding ($R(\lambda)$) for each wavelength λ was defined according to the recorded maximum pressure values as the following.

$$R(\lambda) = \frac{\max(p_{1,\lambda})}{\max(p_{0,\lambda})} \quad (16)$$

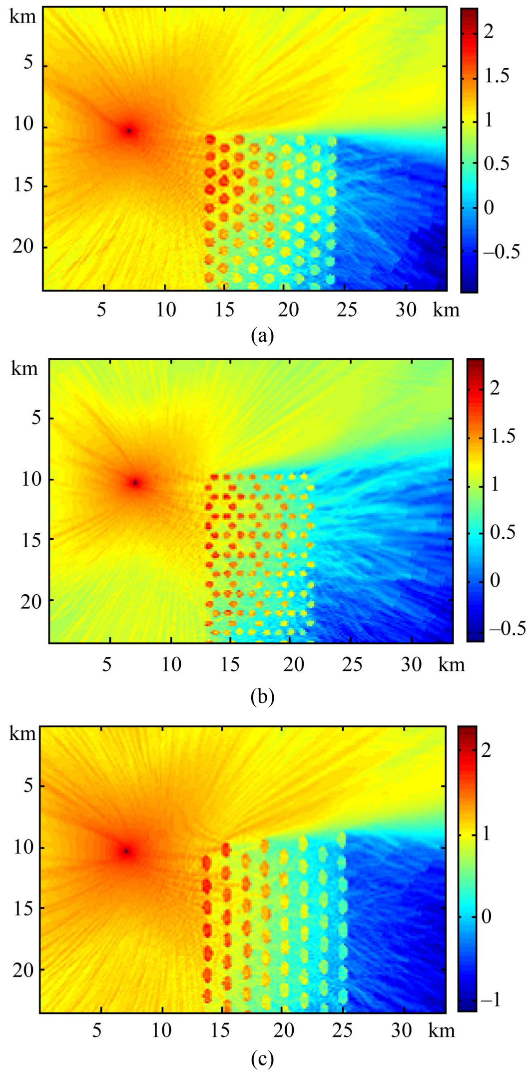

Figure 7. Maximum granule acceleration map in logarithmic scale.

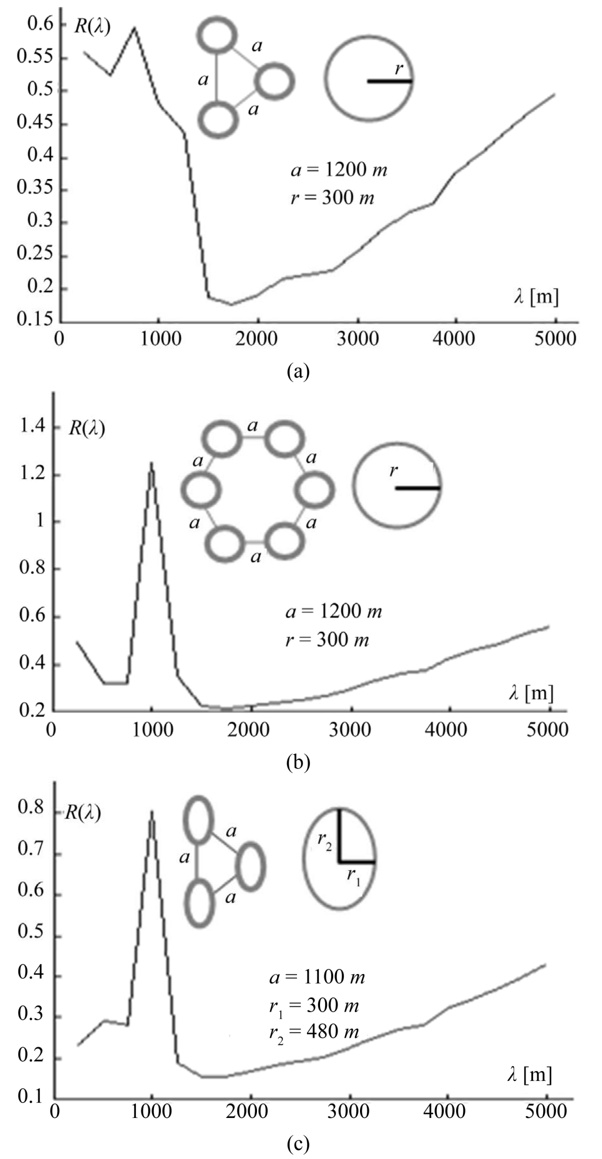

Figure 8. (a) Reduction rate for triangular lattice configuration with circular scatterer; (b) Reduction rate for honeycomb lattice configuration with circular scatterer; (c) Reduction rate for triangular lattice configuration with elliptic scatterer.

In **Figures 8(a)-(c)**, maximum pressure reduction rates versus wavelength (λ) were drawn for the various seismic crystals. The seismic crystals are seen to be capable of providing a seismic attenuation at the wavelength band between nearly 1500 m and 3000 m.

3. Conclusions

In this paper, a possible seismic crystal application with the sizes of kilometers was investigated in an analogy with the acoustic band gaps of phononic and sonic crystals. Their possible applications to seismic wave attenuation were numerically demonstrated by means of FDTD based simulations and their possible application to earthquake shielding was theoretically discussed for various lattice configurations. We observed from the simulation results that the proposed seismic crystal can suppress higher frequency components in vibration spectrum of the earthquake and consequently lead to decreasing ground acceleration.

For future study, three dimensional simulation of seismic crystals should be done with more realistic parameters and the real records from earthquakes to better asses performance of earthquake shielding. Although surface wave suppression by full band gaps was theoretically and experimentally demonstrated for the hole scatterers-solid host type phononic crystal, the seismic wave attenuation via enormous size seismic crystals structures needs to be also experimentally demonstrated in future works.

4. References

[1] T. Miyashita, "Sonic Crystals and Sonic Wave-Guides," *Measurement Science and Technology*, Vol. 16, No. 5, 2005, pp. 47-63. doi:10.1088/0957-0233/16/5/R01

[2] X. D. Zhanga and Z. Y. Liu, "Negative Refraction of Acoustic Waves in Two-Dimensional Phononic Crystals," *Applied Physics Letters*, Vol. 85, No. 2, 2004, pp. 341-343. doi:10.1063/1.1772854

[3] M. M. Sigalas, "Theoretical Study of Three Dimensional Elastic Band Gaps with the Finite-Difference Time-Domain Method," *Journal of Applied Physics*, Vol. 87, No. 6, 2000, pp. 3122-3125. doi:10.1063/1.372308

[4] T. Miyashita and C. Inoue, "Numerical Investigations of Transmission and Waveguide Properties of Sonic Crystals by Finite-Difference Time-Domain Method," *Japanese Journal of Applied Physics*, Vol. 40, 2001, pp. 3488-3492. doi:10.1143/JJAP.40.3488

[5] M. S. Kushwaha and B. Djafari-Rouhani, "Sonic-Stop bands for periodic Arrays of Metallics Rods: Honeycomb Structure," *Journal of Sound and Vibration*, Vol. 218, No. 10, 1998, pp. 697-709. doi:10.1006/jsvi.1998.1839

[6] M. Hirsekorn, "Small-Size Sonic Crystals with Strong Attenuation Bands in the Audible Frequency Range," *Applied Physics Letters*, Vol. 84, No. 17, 2004, p.3364. doi:10.1063/1.1723688

[7] E. N. Economou and M. M. Sigalas, "Classical Wave Propagation in Periodic Structures: Cermet versus Network Topology," *Physical Reviews B*, Vol. 48, No. 18, 1993, pp. 13434-13438. doi:10.1103/PhysRevB.48.13434

[8] N. K. Batra, P. Matic and R. K. Everett, "Sonic Crystal Composites for Selective Noise Reduction," *Proceedings of IEEE Ultrasonic Symposium*, Vol. 1, 8-11 October 2002, pp. 547-550.

[9] E. Ozbay, K. Guven, K. Aydin, "Metamaterials with Negative Permeability and Negative Refractive Index: Experiments and Simulations," *Journal of Optics A*: *Pure Applied Optics*, Vol. 9, No. 9, 2007, pp. S301-307. doi:10.1088/1464-4258/9/9/S04

[10] J. Sun, C. C. Chan, X. Y. Dong and P. Shum, "Tunable Photonic Band Gaps in a Photonic Crystal Fiber Filled with Low Index Material," *Journal of Optoelectronics and Advanced Materials*, Vol. 8, 2006, pp. 1593-1596.

[11] E. Yablonovitch, "Photonic Band-Gap Crystals," *Journal of Physical Condensed Matter*, Vol. 5, No. 16, 1993, p. 2443. doi:10.1088/0953-8984/5/16/004

[12] M. Ciobanu, L. Preda, A. Popescu, M. Mihailescu and M. I. Rusu, "Designing Tunable Photonic Crystals with Band Gaps in Microwave Range," *Journal of Computational and Theoretical Nanoscience*, Vol. 7, No. 6, 2010, pp. 1032-1034. doi:10.1166/jctn.2010.1449

[13] F. Meseguer, M. Holgado, D. Caballero, N. Benaches, C. Lopez, J. Sanchez-Dehesa and J. Llinares, "Two-Dimensional Elastic Bandgap Crystal to Attenuate Surface Waves," *Journal of Lightwave Technology*, Vol. 17, No. 11, 1999, pp. 2196-2201. doi:10.1109/50.803011

[14] F. Meseguer, M. Holgado, D. Caballero, N. Benaches, J. S'anchez-Dehesa, C. L'opez, and J. Llinares, "Attenuation of Surface Elastic Waves (Earthquakes) by Phononic Crystals," *Physical Reviews B*, Vol. 59, No. 19, 1999, pp. 12169-12172. doi:10.1103/PhysRevB.59.12169

[15] S. Benchabane, A. Khelif, J. Y. Rauch, L. Robert and V. Laude, "Evidence for Complete Surface Wave Band Gap in a Piezoelectric Phononic Crystal," *Physical Reviews E*, Vol. 73, No. 6, 2006, p. 065601(4). doi:10.1103/PhysRevE.73.065601

[16] V. Laude, M. Wilm, S. Benchabane and A. Khelif, "Full Band Gap for Surface Acoustic Waves in a Piezoelectric Phononic Crystal," *Physical Reviews E*, Vol. 71, No. 3, 2005, p. 036607(7). doi:10.1103/PhysRevE.71.036607

[17] Y. Tanaka and S. Tamura, "Two-Dimensional Phononic Crystals: Surface Acoustic Waves," *Physica B*: *Condensed Matter*, Vol. 263-264, 1999, pp. 77-80. doi:10.1016/S0921-4526(98)01197-1

[18] R. Martınez-Salaa, C. Rubioa, L. M. Garcia-Raffib, J. V. Sanchez-Pereza, E. A. Sanchez-Pereza and J. Linaresa, "Control of Noise by Trees Arranged Like Sonic Crystals," *Journal of Sound and Vibration*, Vol. 291, No. 1-2, 2006, pp. 100-106. doi:10.1016/j.jsv.2005.05.030

[19] J. V. Sanchez, D. Caballero, R. Martinez-Sala, C. Rubio, J. Sanchez-Dehesa, F. Meseguer, J. Llinares and F. Galvez, "Sound Attenuation by Two-Dimensional Array of Rigid Cylinders," *Applied Physics Letters*, Vol. 80, No. 24, 1998, pp. 5325-5328. doi:10.1103/PhysRevLett.80.5325

[20] M. Brun, S. Guenneau and A. B. Movchan, "Achieving Control of In-Plane Elastic Waves," *Applied Physics Letters*, Vol. 94, No. 6, 2009, p. 061903(3). doi:10.1063/1.3068491

[21] M. Farhat, S. Guenneau and S. Enoch, "Ultrabroadband Elastic Cloaking in Thin Plates," *Applied Physics Letters*, Vol. 103, No. 2, 2009, p. 024301(4). doi:10.1103/PhysRevLett.103.024301

[22] L. Y. Wu and L. W. Chen, "The Dispersion Characteristics of Sonic Crystals Consisting of Elliptic Cylinders," *Journal of Physics D*: *Applied Physics*, Vol. 40, No. 23, 2007, pp. 7579-7583. doi:10.1088/0022-3727/40/23/051

[23] C. Qiu, X. Zhang and Z. Liu, "Far-Field Imaging of Acoustic Waves by a Two-Dimensional Sonic Crystal," *Phys Reviev B*, Vol. 71, No. 5, 2005, p. 054302(6). doi:10.1103/PhysRevB.71.054302

[24] S. Alagoz and B. B. Alagoz, "Frequency-Controlled Wave Focusing by a Sonic Crystal Lens," *Applied Acoustics*, Vol. 70, No. 11-12, 2009, pp. 1400-1405. doi:10.1103/PhysRevB.71.054302

[25] L. E. Kinsler, A. R. Frey, B. Coppens and J. V. Sanders, "Fundamentals of Acoustics," John Wiley & Sons Inc., New York, 1982.

